

RESEARCH ARTICLE



WILEY

Development and improvement of a transient temperature model of PV modules: Concept of trailing data

Whyte Goodfriend^{1,2} | E. Bart Pieters¹ | Merdzhanova Tsvetelina¹ |
Agbo Solomon¹ | Fabian Ezema² | Uwe Rau^{1,3}

¹IEK-5 Photovoltaik, Forschungszentrum Jülich GmbH, Jülich, Germany

²Department of Physics and Astronomy, University of Nigeria Nsukka, Enugu, Nigeria

³Jülich Aachen Research Alliance (JARA-Energy) and Faculty of Electrical Engineering and Information Technology, RWTH Aachen University, Aachen, Germany

Correspondence

Whyte Goodfriend, IEK-5 Photovoltaik, Forschungszentrum Jülich GmbH, Wilhelm-Johnen Straße, Jülich 52425, Germany.
Email: g.whyte@fz-juelich.de

Funding information

Bundesministerium für Bildung und Forschung, Grant/Award Numbers: 03EW0001C, 03SF0576A-B

Abstract

The development of a transient temperature model of photovoltaic (PV) modules is presented in this paper. Currently, there are a few steady-state temperature models targeted at assessing and predicting the PV module temperature. One of the most commonly used models is the Faiman thermal model. This model is derived from the modified Hottel-Whillier-Bliss (HWB) model for flat-plate solar-thermal collector under steady-state conditions and assumes low or no thermal mass in the modules (i.e., short time constants such that transients are neglected, and steady-state conditions are assumed). The transient extension of the Faiman model we present in this paper introduces a thermal mass, which provides two advantages. First of all, it improves the temperature prediction under dynamic conditions. Second, our transient extension to the Faiman model allows the accurate parametrization of the Faiman model under dynamic conditions. We present our model and parametrization method. Furthermore, we applied the model and parametrization method to a 1-year data set with 5-min resolved outdoor module measurements. We demonstrate a significant improvement in temperature prediction for the transient model, especially under dynamic conditions.

KEYWORDS

module temperature, PV modules, steady-state model, thermal model, transient model

1 | INTRODUCTION

The accurate determination of the operating temperature of PV modules, especially operated under outdoor conditions, is of key importance in the field of photovoltaics. This is, among other reasons, due to the critical dependence of the PV yield on temperature.^{1–8} Thus, module temperature prediction attracts considerable research interests in the recent decade.^{9–14} Moreover, two important quantities in photovoltaics: the Climatic Energy Rating of PV modules (CSER) according to International Electrotechnical Commission (IEC) 61853-3 standard series¹⁵ and the Nominal Module Operating Temperature (NMOT),^{16,17}

require an accurate module temperature prediction. These quantities depend heavily on the standard Faiman temperature model.

The Faiman model is widely used as it is very simple, using linearized effective heat loss, and for many applications adequate.^{4,7,15,18} However, the model neglects the thermal mass of the PV module and thus neglects transients. This makes the Faiman model, like every other steady-state model, inaccurate under rapidly changing conditions.^{11,19,20} Furthermore, the inability to accurately describe temperature transients hampers model parametrization as measured data must be filtered to only select those datapoints where the conditions were sufficiently stable to assume a steady-state temperature.¹⁶

This is an open access article under the terms of the [Creative Commons Attribution](https://creativecommons.org/licenses/by/4.0/) License, which permits use, distribution and reproduction in any medium, provided the original work is properly cited.

© 2024 The Authors. Progress in Photovoltaics: Research and Applications published by John Wiley & Sons Ltd.

One way to overcome this limitation of the Faiman model is to extend it to a transient thermal model. Various transient thermal models have been developed.^{11,13,20–26} However, these models are generally much more complex than the Faiman model, distinguishing between convective and radiative heat loss and applying nonlinear heat loss terms.

In this work, we propose a simple transient extension of the Faiman model with only one extra parameter for the thermal mass of the module. The model is compatible with the Faiman model such that the transient extension may be used to obtain a parametrization for the original steady-state model. This allows us to parameterize both the Faiman model as well as our extension thereof, without the usual data filtering to reject datapoints where the conditions are too dynamic. We demonstrate that our model provides a significant improvement in temperature prediction over the Faiman model, in particular under dynamic conditions.

In Section 2, we briefly present the source and composition of the dataset used in the model development and the parametrization approach of the Faiman model. In Section 3, our proposed model and its parametrization are introduced. We compare our transient model with the Faiman model for all the datasets and further show the significant improvement realized by our model when we focus only on dynamical conditions. Finally, we summarize the key findings of our work in Section 4.

2 | DATA SOURCE AND THEORY

2.1 | Data description

The dataset used in this work was collected from a PV test facility in Widdershall, in the south of Germany. The data set includes the module temperature (T_m) and weather data. The weather data consists of the plane of array (POA) irradiance (G), wind speed (w), and rack ambient temperature (T_a). The data have a temporal resolution of 5 min, collected over the year 2015. Exploratory data analysis was conducted on the dataset to filter out missing sensor data. The resulting data set consists of 78,777 complete measurements.

2.2 | Parametrization of Faiman model

The Faiman model in its original form²⁷ is given by the interdependence of the module temperature T_m on the ambient temperature T_a given by

$$T_m = T_a + G/(u_0 + u_1 w), \quad (1)$$

where T_m (K) is the module temperature, T_a (K) is the ambient temperature, G (W/m²) is the irradiance, w is the wind speed, and u_0 (W/[m² K]) is a convective heat loss term, and u_1 (Ws/[m³ K]) describes the wind dependent forced convection.

Usually, the model is parameterized using linear least squares fit of

$$u_0 + u_1 w = G/(T_m - T_a). \quad (2)$$

According to the IEC 61853-2 standard,²⁸ prior to the linear fitting to determine the model parameters, a minimum of 10 days high frequency measurements taken on a suitably clear day is usually required. Furthermore, the input data are preprocessed by rejecting certain data points to achieve steady-state conditions as much as possible. Consequently, the following filtering procedure is followed²⁸:

- Data points with irradiance values below 400 W/m² are rejected.
- Irradiance values fluctuating more than $\pm 10\%$ from the maximum to the minimum value within 10 min interval are also rejected.
- Instantaneous windspeed data with a deviation below 0.25 m/s or wind gusts above +200% from a 5 min running average within 10 min interval are rejected.
- After rejecting gusts and low wind speeds, all data when the 5 min running average is less than 1 m/s or greater than 8 m/s are also rejected.

Unfortunately, this data filtering procedure poses a strict reduction in the number of usable data points for analysis. In fact, other researchers have clearly noted that only about 0.3% of data points are usable after filtering.¹⁶ Furthermore, wind speed ranges with higher point density exert more weights in the regression, leading to a lower regression accuracy.¹⁶

As we cannot strictly follow the Faiman parametrization procedure according to the IEC norm due to the low resolution of our dataset, we parameterize the Faiman model using an equivalent form given by

$$(T_m - T_a)(u_0 + u_1 w) = G. \quad (3)$$

This equivalent form is more robust to numerical errors in case $(T_m - T_a)$ is small. The parameters determined from this approach as well as the predicted temperature plots are presented in Figure 1.

Note that by applying linear least squares on Equations (2) and (3), the parameters u_0 and u_1 are determined such that the errors in the right-hand side of the equations are minimized. It should be noted that this is generally not identical to the solution where the error in the module temperature is minimized.

2.3 | Transient model development

We propose the following differential equation for a transient temperature model:

$$C_a \frac{dT_m}{dt} = G - (u_0 + u_1 w)(T_m - T_a), \quad (4)$$

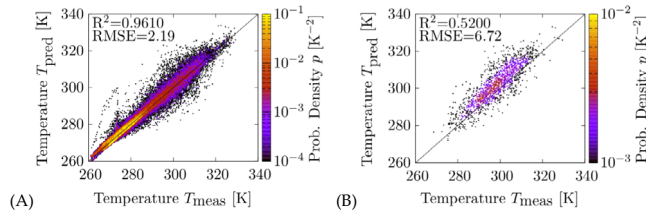


FIGURE 1 Scatter density plots for the predicted temperature (T_{pred}) versus the measured temperature (T_{meas}). The color of the scatter points shows the estimated density of scatter points in logarithmic scale. (a) the Faiman model prediction for the whole dataset. (b) Model prediction for a filtered dataset where $|\Delta T_m| > 2^\circ\text{C}$, that is, select only those points where two subsequent temperature measurements show a large difference.

where C_a ($\text{J}/(\text{m}^2 \text{K})$) is the area-specific thermal capacitance; that is, it is the heat capacity per unit area, and all other parameters are as earlier defined.

Under the assumption that the irradiance, wind, and ambient temperature do not vary, this differential equation has an analytical solution of the form

$$T_m(t) = T_{ss} - C \exp[-t(u_0/C_a + u_1 w/C_a)], \quad (5)$$

where

$$T_{ss} = T_a + G/(u_0 + u_1 w), \quad (6)$$

$$C = T_{ss} - T_m(0). \quad (7)$$

Also, under steady-state conditions, Equation (5) reduces to Equation (6), with $T_m = T_{ss}$, where T_{ss} is the module temperature at steady-state. Note that Equation (6) is the Faiman equation as in Equation (1), with $T_m = T_{ss}$. Thus, a parametrization of the Faiman model is directly obtained from our model parameters.

2.4 | Parametrization approach

We parameterize our transient model from a time series of data points (G_i , $T_{a,i}$, w_i , and $T_{m,i}$) to determine the parameters, u_0 , u_1 , and C_a , by considering time intervals between consecutive data points. Consequently, we employ the finite difference approach while assuming constant conditions within an interval $[t_i, t_{i+1}]$. A good choice for the constant value would be the first order approximation of the value in the center of each interval: $X_{i+0.5} = (X_i + X_{i+1})/2$, where X is substituted with one of the quantities G , T_a , w , T_m , and i is the time series measurement index ($i = 1 \dots N$), and $t_i < t_{i+1}$ for all i , and N is the number of measurements in the time series. Hence, we linearize Equation (4) to obtain Equation (8) as

$$G_{i+0.5} - (u_0 + u_1 w_{i+0.5})(T_{m,i+0.5} - T_{a,i+0.5}) = C_a \frac{T_{m,i+1} - T_{m,i}}{t_{i+1} - t_i}. \quad (8)$$

To compute the temperature at a specific time, we consider the thermal history of the module by trailing back in time. Here, we simply assume that we have a steady-state condition at $t - \Delta t_i$ minutes, where Δt_i is the trailing time. We numerically integrate Equation (8) up to the desired time to get the module temperature, $T_m(t)$. The simplified process flow is as follows:

- I.) At $t - \Delta t_i$ minutes, we assume steady-state conditions, that is, $T_m(t - \Delta t_i) = T_{ss}(t - \Delta t_i)$,
- II.) We compute the temperature for the next time step ($T_{m,i+1}$), using

$$T_{m,i+1} = T_{m,i} + \Delta t_i / C_a [G_{i+0.5} - (u_0 + u_1 w_{i+0.5})(T_{m,i} - T_{a,i+0.5})]. \quad (9)$$

- III.) The final module temperature at time t is obtained by integrating N time steps using Equation (9), where

$$\Delta t_t = \sum_{i=0}^N \Delta t_i. \quad (10)$$

3 | RESULTS AND DISCUSSIONS

3.1 | Faiman model results

The ordinary least squares fitting was done using the equivalent equation of the Faiman model in Equation (3), for all the dataset, which yielded the Faiman parameters, u_0 and u_1 as $29.66 \text{ Wm}^{-2} \text{K}^{-1}$ and $5.64 \text{ Wm}^{-3} \text{sK}^{-1}$, respectively. These values are comparable to those obtained by other authors in the literature.^{16,27} The Faiman parameters are subsequently used in Equation (1) to predict the module temperature, and the plots are presented in Figure 1.

Figure 1a shows a scatter density plot for the measured versus the Faiman predicted module temperature (T_m). The color scale depicts the density of points in the scatter plot (note the logarithmic scale). Large density of points especially at low temperatures is reasonably well predicted by the model. However, for these points, the irradiance is generally low, and thus, the module temperature is close to the ambient temperature. At higher temperatures, the scatter fans out a bit. Nevertheless, the plot clearly depicts that even without data filtering and other extraneous data preprocessing, the Faiman model works fairly well. The coefficient of determination, R^2 , and the root-mean-square error, RMSE, are 0.9610 and 2.19 K, respectively.

We expect the Faiman model to be less accurate under dynamic conditions. To show this, we filter our dataset by selecting datapoints where the magnitude of ΔT_m for the preceding interval is greater than 2°C ($|\Delta T_m| > 2^\circ\text{C}$); that is, we select those points in the dataset where the temperature is rapidly changing. The predicted versus the measured module temperatures for the thus filtered dataset is shown in Figure 1b. It is clearly seen that during these dynamic moments, the model is much less accurate with an R^2 value of 0.5200 and an RMSE of 6.72 K, which is more than a factor 3 larger as compared to the RMSE for the complete dataset. This is seen in the large scatter of points in Figure 2b with only very few points lying on the regression line.

3.2 | Transient model results

In the next step, we parameterize the transient model. In principle, we can use an ordinary least squares (OLS) approach to find the coefficients C_a , u_0 , and u_1 from Equation (8). Figure 2a shows the measured (ΔT_{meas}) and predicted (ΔT_{pred}) temperature difference for subsequent

measurements in the time series ($\Delta T_m = T_{m,i+1} - T_{m,i}$), where the parameters are obtained with OLS. However, we observe that the variance of the residuals is not constant across the ΔT_{meas} .

When non-constant variance of the residuals is observed, it indicates that the variability of the errors is not consistent throughout the data range (in ΔT_{meas}). Moreover, this condition represents a violation of the assumption of homoscedasticity, a critical assumption in linear regression. Consequently, such a violation can introduce bias into parameter estimates and lead to incorrect statistical inferences.^{29–31}

This problem arises from a rather unbalanced dataset where the majority of ΔT_m values are close to 0. To overcome this, we apply a weighted least square (WLS) regression. The weights are obtained by binning the $\Delta T_m/\Delta t$ values into 100 equally spaced bins and set weights inversely proportional to the number of data points per bin. The results of the WLS fit on all the dataset are shown in Figure 2b.

From the parametrization procedure in Equation (8), we obtain the three parameters C_a , u_0 , and u_1 , from the weighted least squares fit as $19.57 \text{ kJ m}^{-2} \text{ K}^{-1}$, $26.31 \text{ W m}^{-2} \text{ K}^{-1}$, and $7.93 \text{ W m}^{-3} \text{ s K}^{-1}$, respectively. The results of the Faiman parameters obtained from our parametrization approach, as well as from the transient model and

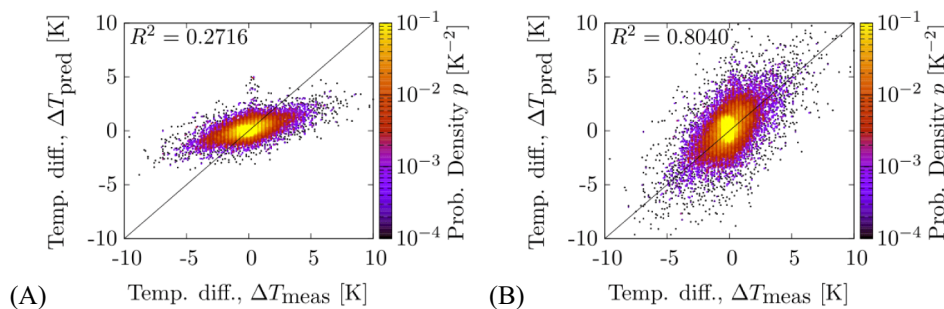


FIGURE 2 Scatter density plots showing the predicted (ΔT_{pred}) versus the measured (ΔT_{meas}) module temperature difference from the transient model parametrization fits using (a) OLS and (b) WLS regression. The solid line is the line of best fits or the identity line for which the modeled and measured ΔT_m are equal, and the color of the scatter points indicates the estimated probability density of the scatter points on a logarithmic scale.

TABLE 1 Values of Faiman parameters derived from equivalent equation, transient model, and published literature.

Faiman parameters	Values from an equivalent equation	Values from our transient model	Values from literature
$u_0 \text{ (W m}^{-2} \text{ K}^{-1}\text{)}$	29.66	26.31	29.27, ²⁸ 32.0 ¹⁶
$u_1 \text{ (W m}^{-3} \text{ s K}^{-1}\text{)}$	5.64	7.93	5.60, ²⁸ 4.5 ¹⁶

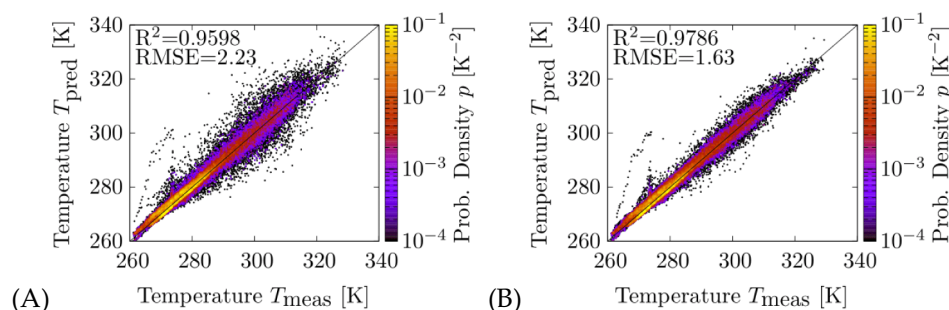


FIGURE 3 Scatter density plots of the predicted temperature (T_{pred}) versus the measured temperature (T_{meas}) for the transient model on all dataset (a) for trail = 0 min (Faiman equivalent) (b) trail = 15 min.

how they compare with literature published values, are shown in Table 1. As compared to the previous direct parametrization of the Faiman model, we observe the new u_0 is slightly smaller (was $29.66 \text{ Wm}^{-2} \text{ K}^{-1}$), whereas the new u_1 is slightly larger (was $5.64 \text{ Wm}^{-3} \text{ sK}^{-1}$). In any case, the exact values of these parameters are no more important than their impact on the annual energy yield for a specific location.²⁸

First, we compare the Faiman model parameterized from the transient model coefficients. In Figure 3a, we show the predicted versus measured module temperature using this alternative parametrization of the Faiman model. The results are nearly identical to Figure 1a. The coefficient of determination and root mean square error are also nearly the same ($R^2 = 0.9598$ and an RMSE = 2.23 K).

The results for the transient model are shown in Figure 3b, where we use a trailing time of 15 min. Here, we observe a better temperature prediction using the transient model, as compared to the Faiman model in Figure 3a. The point cloud gets narrower with more density of data points, which lie about the regression line. The model accuracy improves to having an R^2 value of 0.9786 and RMSE value of 1.63 K. Quantitatively, this RMSE value has been noted in the literature to be comparable to cell-to-cell temperature within any given module.^{4,27} Moreover, in terms of power rating of commonly available PV modules, such as HIT and c-Si modules with typical temperature coefficients of about $-0.3\%/K$ and $-0.5\%/K$, respectively, the RMS error would translate to only 0.48% or 0.82% uncertainty in power.

Next, we evaluate the transient model performance under dynamic conditions. Figure 4 shows plots of filtered datasets for large transients, that is, for moments where the absolute module temperature difference is larger than 2°C ($|\Delta T_m| > 2^\circ\text{C}$).

Figure 4a–c shows the improvement of our transient model from its steady-state counterpart in Figure 1b. In Figure 4a, we show the results without trailing data, which produces more or less identical results as before in Figure 1b, while Figure 4b,c shows results for 5-, 10-, and 15-min trailing data. It is observed that with an increasing trailing time, the model gets more accurate. Under these dynamic conditions, we can reduce the RMSE from 6.69 to 3.33 K.

Similarly, in Figure 5, we show the development of the coefficient of determination and the RMSE, as a function of the trailing time. Figure 5a shows the results for the complete dataset and Figure 5b for the dynamic conditions only. In both figures, we observe that the accuracy improves rapidly up to a trailing time of about 15 min. Trailing further in the past, the less the module temperature is correlated with the current temperature. So if we integrate from a point far in the past, then we get a better temperature estimate.

From Equation (5), we see the time constant τ , for the transients equals $\frac{C_a}{u_0 + u_1 W}$. Using this expression, we compute the average time constant over the entire dataset and obtain 9.74 min. Thus, a 15-min trailing time corresponds to about 1.7 time constants. Note that the time constant for a PV module may vary depending on the module type, mounting construction, and typical wind speeds. Our dataset is for a rack mounted glass module with a back sheet.

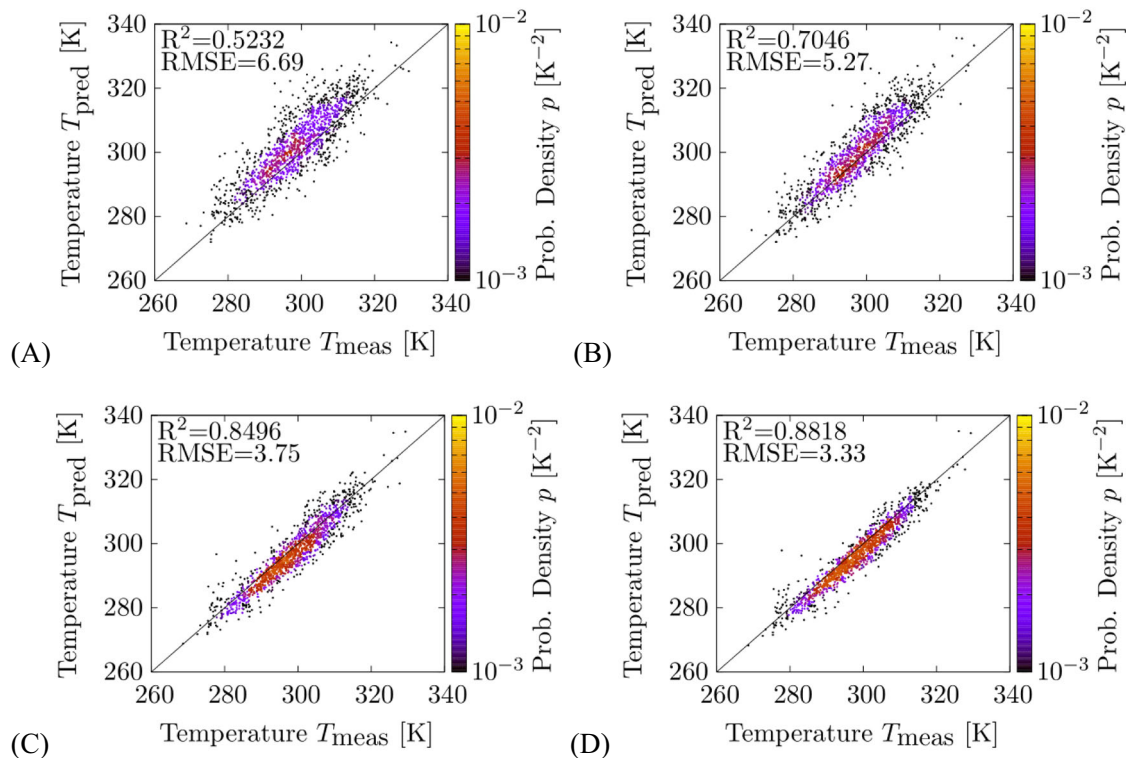


FIGURE 4 Scatter plots showing the results of the transient model for (a) trail = 0 min (Faiman equivalent for filtered data set), (b) trail = 5 min, (c) trail = 10 min, and (d) trail = 15 min.

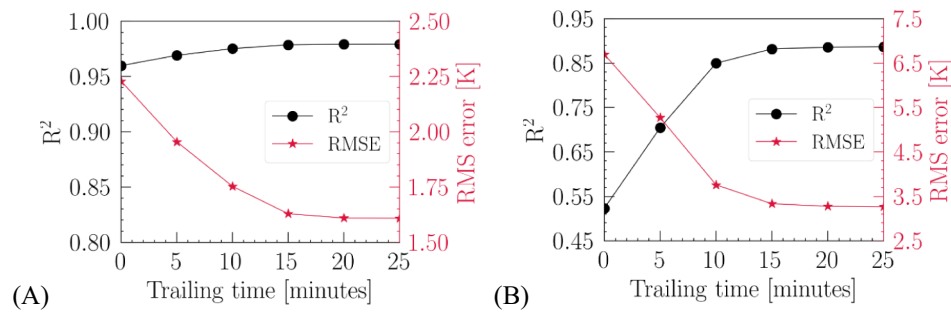


FIGURE 5 Plot of coefficient of determination (R^2) (left axis) and root-mean-square error (RMSE) (right axis) against trailing time in minutes for (a) all dataset and (b) dynamic dataset.

4 | SUMMARY

In this work, we developed a transient extension of the Faiman model. Compared to most published transient models for PV applications, our model is very simple, in line with the Faiman model. Our transient model only adds one more parameter for the thermal mass. Our transient extension to the Faiman model is compatible with the Faiman model in the sense that the models are identical under steady-state conditions, and the standard Faiman parameters can be directly obtained by parametrizing the extended Faiman model. We parametrized our transient model from a time series of data points to determine our model parameters. In principle, our parametrization approach allows the accurate parametrization of both the Faiman model and its extension without the need to filter data for stable conditions. The Faiman model performs well under fairly constant conditions; however, as expected, we observe a significant reduction in model accuracy for those time instances where the module temperature rapidly changes. Our transient extension to the Faiman model achieves a much better accuracy, especially under dynamic conditions. We show that we can accurately model the module temperature in a time series by considering a 15-min thermal history, which corresponds to approximately 1.7 time constants.

ACKNOWLEDGEMENTS

This work has received great sponsorship and funding from the German Federal Ministry of Education and Research (Bundesministerium für Bildung und Forschung, BMBF) under the YESPV-NIGBEN-CLIENT II project (BMBF Förderkennzeichen 03SF0576A-B) and H2ATLAS-AFRICA project (03EW0001C). Open Access funding enabled and organized by Projekt DEAL.

CONFLICT OF INTEREST

The authors declare that they have no known competing financial interest or personal relationships that could have appeared to influence the work reported in this paper.

AUTHOR CONTRIBUTIONS

Whyte Goodfriend: Conceptualization; methodology; data analysis; original draft writing; reviewing & editing. **Bart Pieters:** Conceptualization; methodology; data analysis; reviewing & editing. **Merdzhanova Tsvetelina:** Reviewing & editing; supervision. **Agbo Solomon:**

Reviewing & editing. **Uwe Rau:** Supervision; review & editing. **Ezema Fabian:** Supervision; review & editing.

DATA AVAILABILITY STATEMENT

Research data are not shared.

ORCID

Whyte Goodfriend <https://orcid.org/0000-0002-5152-095X>

E. Bart Pieters <https://orcid.org/0000-0001-6533-2098>

Fabian Ezema <https://orcid.org/0000-0002-4633-1417>

Uwe Rau <https://orcid.org/0000-0003-3526-3081>

REFERENCES

- Skoplaki E, Palyvos JA. On the temperature dependence of photovoltaic module electrical performance: a review of efficiency/power correlations. *Sol Energy*. 2009;83(5):614-624. doi:10.1016/j.solener.2008.10.008
- Ye Z, Nobre A, Reindl T, Luther J, Reise C. On PV module temperatures in tropical regions. *Sol Energy*. 2013;88:80-87. doi:10.1016/j.solener.2012.11.001
- Saber EM, Lee SE, Manthapuri S, Yi W, Deb C. PV (photovoltaics) performance evaluation and simulation-based energy yield prediction for tropical buildings. *Energy*. 2014;71:588-595. doi:10.1016/j.energy.2014.04.115
- Barykina E, Hammer A. Modeling of photovoltaic module temperature using Faiman model: sensitivity analysis for different climates. *Sol Energy*. 2017;146:401-416. doi:10.1016/j.solener.2017.03.002
- Schweiger M, Herrmann W, Gerber A, Rau U. Understanding the energy yield of photovoltaic modules in different climates by linear performance loss analysis of the module performance ratio. *IET Renew Power Gener*. 2017;11(5):558-565. doi:10.1049/iet-rpg.2016.0682
- Liao W, Heo Y, Xu S. Evaluation of temperature dependent models for PV yield prediction, in Proceedings of the 4th Building Simulation and Optimization Conference, Cambridge, UK, 2018; 11-12.
- Driesse A, Theristis M, Stein JS. PV module operating temperature model equivalence and parameter translation, in 49th Photovoltaic Specialist Conference (PVSC), Philadelphia, PA, USA, 2022.
- Schwingshackl C, Petitta M, Wagner JE, et al. Wind effect on PV module temperature: analysis of different techniques for an accurate estimation. *Energy Procedia*. 2013;40:77-86. doi:10.1016/j.egypro.2013.08.010
- Perović B, Klimenta D, Jevtić M, Milovanović M. An analytical model for estimating the temperature of a photovoltaic module based on the principle of energy balance. *Zbornik MKOIEE*. 2017;5(1):89-95.
- Olukan TA, Emziane M. A comparative analysis of PV module temperature models. *Energy Procedia*. 2014;62:694-703. doi:10.1016/j.egypro.2014.12.433

11. Jones A, Underwood C. A thermal model for photovoltaic systems. *Sol Energy*. 2001;70(4):349-359. doi:[10.1016/S0038-092X\(00\)00149-3](https://doi.org/10.1016/S0038-092X(00)00149-3)
12. Luketa-Hanlin A, Stein J. Improvement and validation of a transient model to predict photovoltaic module temperature, Sandia National Laboratories (SNL), Albuquerque, NM, and Livermore, CA, 2012.
13. Jaszczur M, Hassan Q, Szubel M, Majewska E. Fluid flow and heat transfer analysis of a photovoltaic module under varying environmental conditions. *J Phys Conf*. 2018;1101(1):012009. IOP Publishing.
14. Skoplaki E, Palyvos JA. Operating temperature of photovoltaic modules: a survey of pertinent correlations. *Renew Energy*. 2009;34(1):23-29. doi:[10.1016/j.renene.2008.04.009](https://doi.org/10.1016/j.renene.2008.04.009)
15. IEC. IEC 61853-3 Ed. 1.0: Photovoltaic (PV) module performance testing and energy rating—part 3: energy rating of PV modules, 2018; 6–13.
16. Herrmann W, Monokroussos C, Lee K. Comparison of different approaches to determine the nominal PV module operating temperature (NMOT), in Paper presented at 38th European Photovoltaic Solar Energy Conference and Exhibition, 2021; 6: 10.
17. Koehl M, Heck M, Wiesmeier S, Wirth J. Modeling of the nominal operating cell temperature based on outdoor weathering. *Sol Energy Mater Sol Cells*. 2011;95(7):1638-1646. doi:[10.1016/j.solmat.2011.01.020](https://doi.org/10.1016/j.solmat.2011.01.020)
18. Koehl M, Hamperl S, Heck M. Effect of thermal insulation of the back side of PV modules on the module temperature. *Prog Photovolt: Res Appl*. 2016;24(9):1194-1199. doi:[10.1002/pip.2773](https://doi.org/10.1002/pip.2773)
19. Kratochvil JA, Boyson WE, King DL. Photovoltaic array performance model, Sandia National Laboratories (SNL), Albuquerque, NM, and Livermore, CA, 2004.
20. Lobera DT, Valkealahti S. Dynamic thermal model of solar PV systems under varying climatic conditions. *Sol Energy*. 2013;93:183-194. doi:[10.1016/j.solener.2013.03.028](https://doi.org/10.1016/j.solener.2013.03.028)
21. Perovic B, Klimenta D, Jevtic M, Milovanovic M. A transient thermal model for flat-plate photovoltaic systems and its experimental validation. *Elektron ir Elektrotehnika*. 2019;25(2):40-46. doi:[10.5755/j01.eie.25.2.23203](https://doi.org/10.5755/j01.eie.25.2.23203)
22. Mattei M, Notton G, Cristofari C, Muselli M, Poggi P. Calculation of the polycrystalline PV module temperature using a simple method of energy balance. *Renew Energy*. 2006;31(4):553-567. doi:[10.1016/j.renene.2005.03.010](https://doi.org/10.1016/j.renene.2005.03.010)
23. Armstrong S, Hurley WG. A thermal model for photovoltaic panels under varying atmospheric conditions. *Appl Therm Eng*. 2010;30(11):1488-1495. doi:[10.1016/j.applthermaleng.2010.03.012](https://doi.org/10.1016/j.applthermaleng.2010.03.012)
24. Notton G, Cristofari C, Mattei M, Poggi P. Modelling of a double-glass photovoltaic module using finite differences. *Appl Therm Eng*. 2005;25(17):2854-2877. doi:[10.1016/j.applthermaleng.2005.02.008](https://doi.org/10.1016/j.applthermaleng.2005.02.008)
25. Trinuruk P, Sorapipatana C, Chenvidhya D. Estimating operating cell temperature of BIPV modules in Thailand. *Renew Energy*. 2009;34(11):2515-2523. doi:[10.1016/j.renene.2009.02.027](https://doi.org/10.1016/j.renene.2009.02.027)
26. Oh SY, Kim MS, So WS, et al. Outdoor operating temperature modeling of photovoltaic modules including transient effect, in 2017 IEEE 44th Photovoltaic Specialist Conference (PVSC), 25–30. 2017; 487–489, doi:[10.1109/PVSC.2017.8366327](https://doi.org/10.1109/PVSC.2017.8366327).
27. Faiman D. Assessing the outdoor operating temperature of photovoltaic modules. *Prog Photovolt: Res Appl*. 2008;16(4):307-315. doi:[10.1002/pip.813](https://doi.org/10.1002/pip.813)
28. IEC. IEC 61853-2 Ed. 1.0: Photovoltaic (PV) module performance testing and energy rating—part 2: spectral responsivity, incidence angle and module operating temperature measurements. 2016; 17–19.
29. Frost J. 7 Classical assumptions of ordinary least squares (ols) linear regression. Statistics By Jim. <https://statisticsbyjim.com/regression/ols-linear-regression-assumptions/> (accessed September 27, 2023).
30. Frost J. Heteroscedasticity in regression analysis. Statistics by Jim. <https://statisticsbyjim.com/regression/heteroscedasticity-regression/> (accessed September 27, 2023).
31. Frost J. *Regression Analysis: An Intuitive Guide for Using and Interpreting Linear Models*. Statistics By Jim Publishing; 2020.

How to cite this article: Goodfriend W, Pieters EB, Tsvetelina M, Solomon A, Ezema F, Rau U. Development and improvement of a transient temperature model of PV modules: Concept of trailing data. *Prog Photovolt Res Appl*. 2024;32(6):399-405. doi:[10.1002/pip.3785](https://doi.org/10.1002/pip.3785)